Sensors & Transducers, Vol. 178, Issue 9, September 2014, pp. 28-33

www.sensorsportal.com

Sensors & Transducers

http://www.sensorsportal.com

Reliability Design about Release Holes in Beam of Fuze MEMS G-Switch

Bo LI, Ya ZHANG, Xiaolin PAN

School of Mechatronics Engineering, North University of China, Taiyuan, 030051, China

Tel.: 86-13834210814, fax: 86-0351-3922285

E-mail: lilancun@163.com

Received: 27 June 2014 /Accepted: 29 August 2014 /Published: 30 September 2014

Abstract: Fuze microstructures include micro acceleration switches, security mechanisms, which the key elements are the elastic elements, such as micro beams, micro springs. Micro material and structure of the elastic element will determine the mechanical properties of the Fuze microstructures. In this paper, optimization design is done for the micro cantilever beam in the Gravity Switches by SOI (silicon on insulator) wafer through design stress release square holes with 10um length of side, leads to an increase in sensitivity and a decrease in crack growth, which meet the requirements of the process reliability and working reliability. *Copyright © 2014 IFSA Publishing, S. L.*

Keywords: MEMS G-Switch, Release holes, Reliability design, Fuze microstructure.

1. Introduction

The Micro-electro mechanical systems (MEMS) Gravity switches (G-Switch) are used for projectiles that carry explosives. A G-Switch of a projectile can close an electrical circuit upon impact that means during the impact there accompanies an acceleration forward which makes two metal pole contacts. MEMS G-Switch is used in safe and arm systems of some Fuzes. MEMS devices are smaller, lighter, more accurate, more reliable, and often cheaper than conventional devices. Materials of the G-Switch in this paper (Fig. 1) were SOI (silicon on insulator) wafer that includes a silicon substrate covered by an insulating layer, silicon dioxide, over which is deposited another silicon device layer, which is the layer from which the moveable parts of the switch will be fabricated. And using Bulk Silicon Processing, micro structures can be etched in one procedure when the micro mass, micro beam, micro spring thickness is equal for, which can got good consistency for the thickness direction for SOI device layer error approximate ± 0.5 um [1-5].

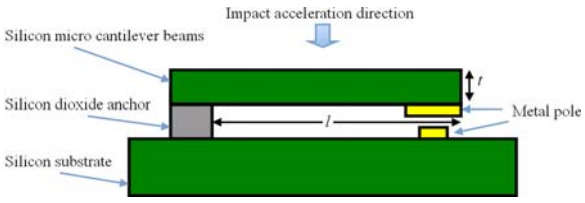

Fig. 1. Cross sections in the up state position of MEMS G-Switch.

2. Mechanical Properties Analysis of Micro Beam of G-Switch

2.1. Cantilever Beams in G-Switch Spring Constant

The first thing in understanding the mechanical operation of MEMS G-Switches is to derive the

spring constant of cantilever beam in G-Switch. If the operation of the cantilever beam is limited to small deflections, as is the case for most MEMS G-Switch, the mechanical behavior of G-Switch can be modeled using a linear spring constant, k (N/m). The deflection, Δx (m), of the cantilever beam for an external force, F (N), can then be obtained using the formula: F =kΔx [6-7].

Micro beam in the SOI G-Switch can be simplified as the cantilever beam model, and inertial force also can be approximated to distributed vertical load, due to a uniform force applied over the entire beam, the expression for the spring constant, k_a, of a cantilever beam in G-Switch is given by [8-9]:

$$k_a = \frac{4EI}{l^3} = \frac{2Ew}{3}(\frac{t}{l})^3 \quad (1)$$

The moment of inertia, *I*, for a rectangular cross section is given by $I = wt^3/12$, where w is the width of the cantilever beam. where t is the thickness and l is the length of the beam.

2.2. Influence Due to Stress Gradients

An unavoidable fruit of SOI wafer is the presence of a stress gradient, due to the use of multiple layers (silicon device layer / buried oxide layer /silicon substrate) in SOI wafer each with a different residual stress component, in the normal direction of cantilever beams.

Since the G-Switch cantilever beam is not fixed at one end, any residual stress within the SOI wafer is released and the spring constant does not contain a residual-stress component. Also, cantilever beams of G-Switch do not have any stretching parts due to the 'free' condition at the tip of the beam.

However, if there is a stress gradient over the cross section of the beam, then the beam will deflect after release, which is an undesirable effect. So, it is important to reduce the stress gradient for it results in positive or negative beam curvature (Fig. 2) [9].

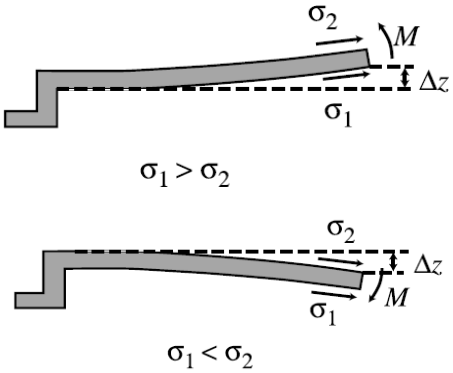

Fig. 2. Effect of stress gradient on cantilever curvature for compressive stress.

The equivalent bending moment due to a stress gradient is

$$M = \int_{-(t/2)}^{t/2} wz\sigma(z)dz, \quad (2)$$

where $\sigma(z)$ is the residual stress as a function of thickness, z is in the thickness direction, and w is the width of the cantilever.

For a linear stress gradient, the stress can be defined as:

$$\sigma(z) = E\Gamma_z, \quad (3)$$

where Γ is the linear strain gradient. Using Eq. 2, can be written as

$$\Gamma = \frac{12M}{Ewt^3} = \frac{M}{EI}, \quad (4)$$

where *I* is the inertia moment of a rectangular beam for $I = wt^3/12$.

A moment applied at the endpoint of the beam with length l results in a deflection at the tip is

$$\Delta z = \frac{Ml^2}{2EI} = \frac{\Gamma l^2}{2} = \frac{6M}{Ew}\left(\frac{l}{t}\right)^2 \quad (5)$$

3. Effect of Release Holes in Beams

When etches are used to release a large microstructural element such as beams, it is common practice to distribute small holes in beams to promote under-etching and release, also for reduction of squeezed-film damping.

In MEMS G-Switches, small diameter holes (3–10 um) are defined in beams to weaken the squeeze film damping and add the switching speed of the MEMS G-Switch. The hole area can be up to about 50 % even to 60 % of the all surface area on the MEMS structure.

The perforation pattern is characterized by the ligament efficiency, $\mu = l/pitch$, which defined as the ratio of the remaining link width to the pattern pitch (Fig. 3) [9].

The holes release certain residual stress in the micro structural, and cut the Young's modulus of the MEMS structure. This has been derived by Senturia's group using 3-D mechanical models [10]. The reduction of the residual stress is approximately equal to $\sigma = (1-\mu)\sigma_0$, where σ_0 is the residual stress with no holes, and the Young's modulus is reduced by 25 % for μ =0.625. The holes also result in a lower mass of the beam, which in turn yields a higher mechanical resonant frequency [10].

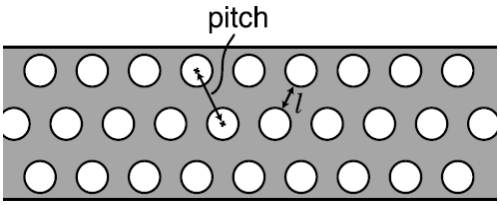

Fig. 3. Parameters for the ligament efficiency in a beam with holes [10].

And a important observations from Fig. 4: smaller area beam have a higher tensile strength since there is a smaller area for pre-exiting cracks or damage, Tensile strength of beam area showing higher fracture strengths when smaller areas are involved, indicating that surface defects rather than volume defects are the initiating points for fracture [11]. So, the beam with holes can narrow beam area will increase tensile strength [13-17].

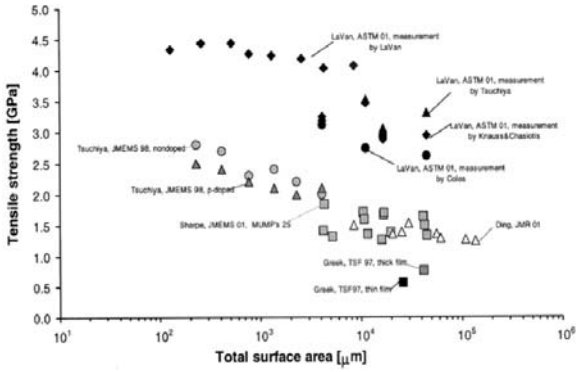

Fig. 4. Tensile strength of polysilicon vs. beam surface area [12].

4. Reliability Design of Release Holes in the Beam

MEMS G-Switch fabricated on SOI wafer need DIRE process what the SOI silicon device layer be etched for expose the buried oxide layer, then the buried oxide layer etched by buffered HF or vapor HF to release free-standing structures (Fig. 5) [18].

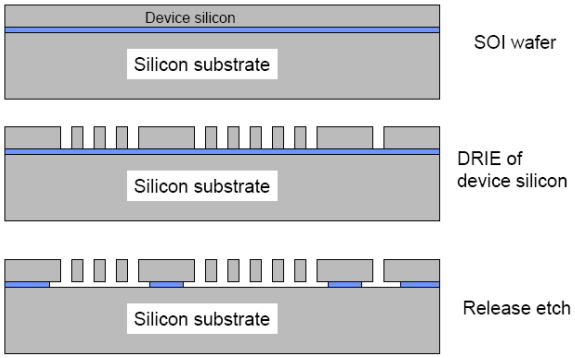

Fig. 5. G-Switch fabricated process on SOI wafer.

G-Switches applied to Fuzes should have the quality of high sensitivity and anti high overload shock. A method to improve the sensitivity of micro switches is to reduce the micro cantilever beam stiffness through change its thickness, length, and width form Eq. 1. While the thickness of micro structure made from SOI equals the device layers in normal conditions which can't be changed usually, so the way is feasible by means of increasing the micro beam length and decreasing its width. But the longer micro beam will increase the size of the whole device is improper thing, then the most convenient way is to narrow the micro beam in the width direction as much as possible. From Fig. 4, the methods to improve the impact resistance is to reduce the surface area of the micro beam, and this can be achieved through arranged holes on the beam, and taken into account the linewidth of DIRE process achieved, in the final design of the device, the micro beam is 30 um width with an array of closely spaced 10 um of square holes as shown in Fig. 6.

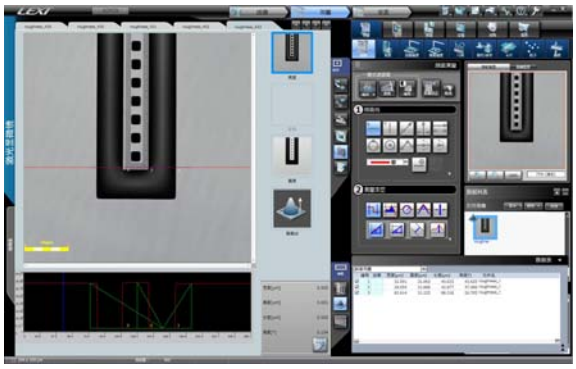

Fig. 6. Photomicrograph of release holes in the beam of the Fuze G-Switch.

5. Simulation on Beam with Release Holes

5.1. Sensitivity Simulation

Due to the number of holes in microstructure is so large that finite element analysis for the entire unit will lead to large amount of calculation even unable to complete. So the sensitivity and linearity simulation and comparison only to part of the porous beam and nonporous beam are carried.

As Fig. 7 and Fig. 8 are displacement nephogram of two kinds of structure, porous and nonporous, in the 150 g acceleration. What can be seen in the same acceleration, the maximum displacement value of the nonporous beam is $4.7184e^{-10}$ m, and the maximum displacement value of the porous beam is $5.6413e^{-10}$ m. The G-Switch is a touch trigger, so offset displacement under the certain acceleration value is a key parameter for sensitivity of G-Switch.

When 20 g-160 g is loaded in the sensitive direction of two beams, the displacement of the mass values are shown in Table 1 and Fig. 9.

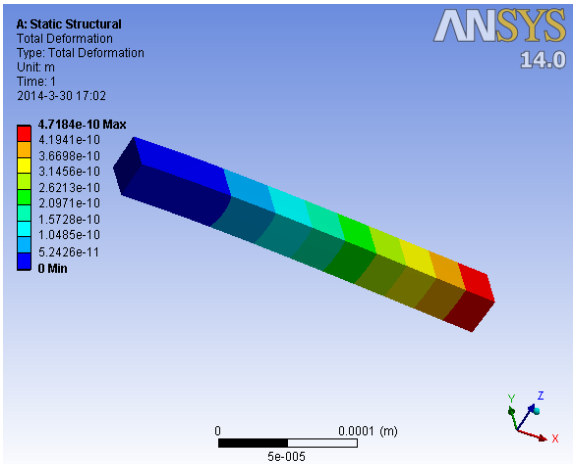

Fig. 7. Displacement nephograph without holes.

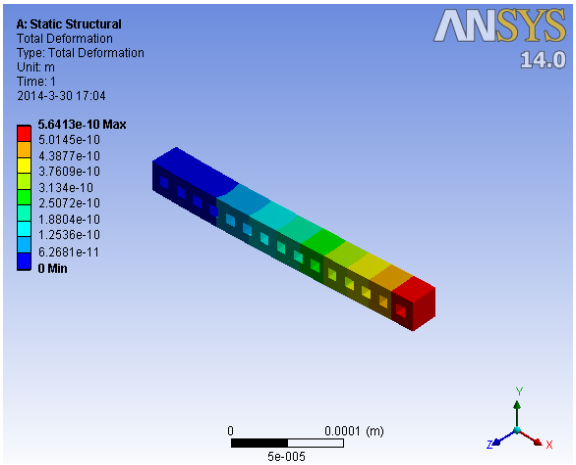

Fig. 8. Displacement nephograph with holes.

Table 1. Displacement of different structure under different acceleration.

	20 g	**40 g**	**60 g**	**80 g**	**100 g**	**120 g**	**140 g**	**160 g**
Beam with holes (x/e^{-10} m)	0.752	1.50	2.26	3.01	3.761	4.513	5.265	6.017
Beam without holes (x/e^{-10} m)	0.629	1.258	1.887	2.516	3.145	3.775	4.404	5.033

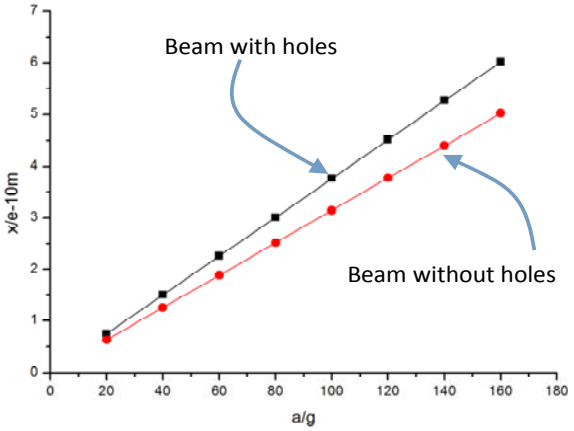

Fig. 9. Displacement of different structure under different acceleration value.

By the above analysis can be concluded that the two kinds of structure has good linear characteristic, and the sensitivity of porous structure is about 1.2 times that of the nonporous structure.

5.2. Mechanical Failure Simulation

When the impact occurred, the joints, scratches and cracks at the beam surface, prone to emerge stress concentration even fracture. But this could be changed by pre-etched holes in beam. Then two kinds of beams were respectively simulated for stress distribution and stress intensity factor by ANSYS under impact stress.

In the etching of silicon micro structure process, micro defects will appear on the surface of the micro structure, will greatly reduce the fracture strength of microstructure, for defects like silicon, the brittle materials, its crack tip stress will concentrate, and not as plastic material can be relax through the deformation. Fracture strength with crack of monocrystalline silicon be derived from the Griffith theory [19-21] from the following formula:

$$\sigma_{ij} = K_{\mathrm{I}} \Big/ (2\pi r)^{\frac{1}{2}} \bullet f_{ij} \tag{6}$$

$$K_{\mathrm{I}} = \sigma(\pi a)^{\frac{1}{2}} \tag{7}$$

Suppose there are infinite width plate, plate center contains length is $2a$ through crack, has two-way pull σ in infinity, from the center of a crack Angle is θ, radius r, point P_{ij}, stress σ_{ij}, and K_I is stress intensity factor, namely the f_{ij} is a factor which associated with the crack position.

Stress nephogram is got under the impact of the 150 g acceleration while the surface crack length is supposed 3 um.

In the process of the analysis of the crack, the stress and strain around the crack is the main object of study, so it is important for the crack tip meshing. Then the crack tip of the grid partition use singular unit, KSCON command, and set the DELR value for the crack length 1/10, PRAT value is 1, NTHET value is 10, KCTIP is Skewed 1/4 pt, selection. And the meshing of the crack territory as shown in Fig. 10 and Fig. 11.

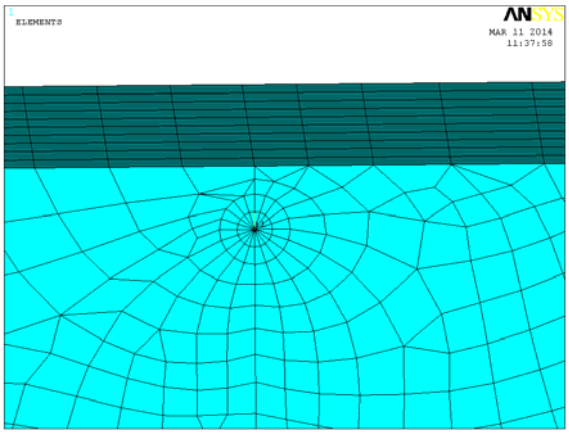

Fig. 10. Crack tip meshing on the beam without holes.

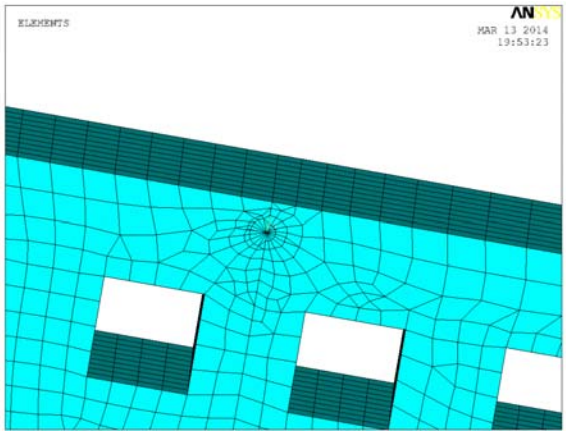

Fig. 11. Crack tip meshing on the beam with holes.

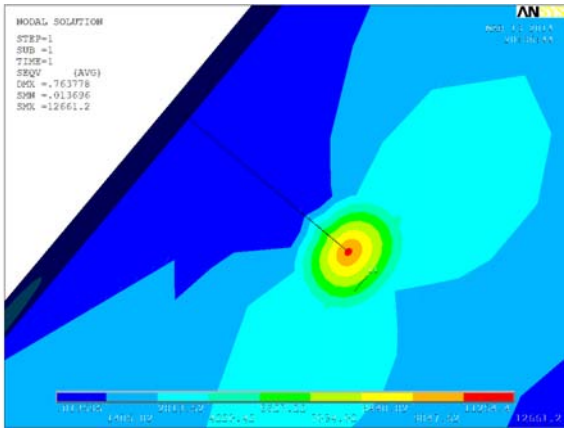

Fig. 12. Stress distribution around the crack on the beam without holes.

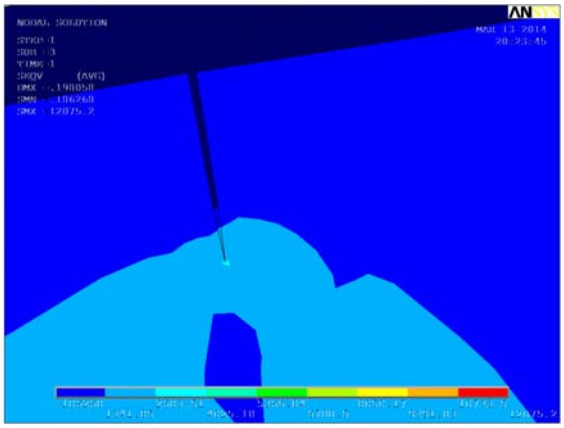

Fig. 13. Stress distribution around the crack on the beam with holes.

As shown in Fig. 12 and Fig. 13 are under the action of 150 g inertial force, the stress distribution around the crack on the two different beams.

It can be seen from the figures: stress concentration at the crack region on the beam without holes, while around the square hole and crack region on beam with holes. Crack tip stress value between 11.25 GPa-12.3 GPa on beam without holes and between 4 GPa-5.4 GPa on beam with holes. For small square holes changed the stress distribution in the beam, reduced the maximum stress, and greatly reduced the crack tip stress value, effectively inhibited crack growth are most likely toprevent Mechanical failure on impact occurs.

In the ANSYS solution is completed, command stream, /POST$PRCINT, 1, K1, input, then two kinds of structure stress intensity values of K1 are got respectively. After analyzing, that is found as Fig. 14 and Fig. 15: The maximum node at the crack tip stress intensity factors K1 for 70742 in the beam without holes, and for 19860 in the beam with holes. The stress intensity factor of the microstructure with holes is greatly reduced, thereby leads to a decrease in crack growth, which raises the reliability of micro structure.

```
***** POST1 K1          RESULT LISTING *****

CrackID =   1
 Crack Front Node =   46
  Contour Values =    70742.       52247.       37847.       -21430.
  Contour Values =   -0.51516E+06
 Crack Front Node = 8860
  Contour Values =    100.38       83.361       65.242       -44.307
  Contour Values =   -709.70
 Crack Front Node = 8861
  Contour Values =    103.26       79.957       61.552       -40.476
  Contour Values =   -705.91
```

Fig. 14. Stress intensity factor list of beam without holes.

```
***** POST1 K1          RESULT LISTING *****

CrackID =   1
 Crack Front Node =    2
  Contour Values =    19860.       11301.       18284.       -67870.
  Contour Values =  -0.37892E+06
 Crack Front Node =22723
  Contour Values =    30.383       19.178       28.570       -87.587
  Contour Values =   -506.70
 Crack Front Node =22724
  Contour Values =    29.580       18.181       27.468       -88.845
  Contour Values =   -507.70
```

Fig. 15. Stress intensity factor list of beam with holes.

6. Conclusions

In Fuze MEMS G-Switches, small diameter holes are made in beams to reduce the squeeze film

damping and increase the switching speed of the MEMS switch.

And the beam with holes have a higher tensile strength for smaller area diminishes pre-exiting cracks or damage, and holes release the residual stress in beams, and reduce the Young's modulus of the MEMS micro structure.

Then the optimization design is done for the micro cantilever beam in the switches by SOI (silicon on insulator) wafer through design stress release square holes with 10 um length of side, leads to an increase in sensitivity and a decrease in crack growth, which meet the requirements of the process reliability and working reliability.

References

[1]. Bo L., Mechanical impact test and analysis based on anti high overload acoustic sensor, *Sens. Lett*., 9, 5, 2011, pp. 1860-1863.

[2]. Bo L., Reliability design to circuit system in hard target smart fuze, *Commun. Comput. Info. Sci*., 144, 2, 2011, pp. 380-384.

[3]. Bo L., Mechanism of parameters variation about electronic components subjected to high impact loads, *Appl. Mech. Mater*., 44, 2011, pp. 256-259.

[4]. Zhang Ya, Xu Jianjun, Zhao Heming, Reliability technology of the ammunition and administration, *Defence Industrial Publishing House*, 2001, pp. 30-60.

[5]. Zhu S.-Y., *et al*., Total dose radiation effects of pressure sensors fabricated on Unibond-SOI materials, *Nucl. Sci. Tech*., 12, 2001, pp. 209-214.

[6]. R. J. Roark, W. C. Young, Formulas for Stress and Strain, 6th edition, *McGraw-Hill*, New York, 1989.

[7]. J. M. Gere, S. P. Timoshenko, Mechanics of Materials, 4th edition, *PWS Publishing Company*, Boston, 1997.

[8]. Yan B. D., Meilink S. L., Warren G. W., Wynblatt P., in *Proc. Electron. Components Conf*., 36, 95, 1986.

[9]. Gabriel M. Rebeiz, RF MEMS Theory, Design, and Technology, *John Wiley & Sons Inc*., 2003, pp. 21-59.

[10]. V. L. Rabinov, R. J. Gupta, S. D. Senturia, The effect of release etch-holes on the electromechanical behavior of MEMS structures, in *Proceedings of the International Conference on Solid-State Sensors Actuators*, Chicago, IL, June 1997, pp. 1125-1128.

[11]. Bagdahn J., Sharpe W. N., Jadaan O., Fracture strength of polysilicon at stress concentrations, *J. Microelectromech. Syst*., 12, 3, 2003, pp. 302–312.

[12]. Allyson L. Hartzell, Mark G. da Silva, Herbert R. Shea, MEMS Reliability, *Springer*, 2011, pp. 85-123.

[13]. Tanner D. M., Walraven J. A., Helgesen K., Irwin L. W., Brown F., Smith N. F., Masters N., MEMS reliability in shock environments, in *Proceedings of the 38th IEEE Int. Reliability Phys. Symp*., 2000, pp. 129-138.

[14]. Sharpe W. N., Bagdahn J., Jackson K., Coles G., Tensile testing of MEMS materials - recent progress, *J. Mater. Sci*., 38, 2003, pp. 4075–4079.

[15]. LaVan D. A., Tsuchiya T., Coles G., Knauss W. G., Chasiotis I., Read D., Cross comparison of direct strength testing techniques on polysilicon films, in Muhlstein C., Brown S. B. (eds), Mechanical Properties of Structural Films, *ASTM STP*, 2001.

[16]. Forehand D. I., Goldsmith C. L., Wafer Level Micropackaging for RF MEMS Switches, in *Proceedings of the ASME InterPACK'05 Tech. Conf.*, San Francisco, CA, July 2005.

[17]. Rebeiz G. M., RF MEMS switches: status of the technology, in *Proceedings of, the 12th International Conference on Solid State Sensors, Actuators and Microsystems (Transducers'03)*, Boston, 8–12 June 2003, pp. 1726.

[18]. Walker J. A., Gabriel K. J., Mehregany M., Mechanical integrity of polysilicon films exposed to hydrofluoric acid solutions, in *Proceedings of the IEEE MEMS*, Napa Valley, CA, 11-14 February 1990, pp. 56–60.

[19]. Zhaoying Zhou, Zhonglin Wang, Liwei Lin, Microsystems and Nanotechnology, *Tsinghua University Press*, 2012.

[20]. Chasiotis I., Knauss W. G., The mechanical strength of polysilicon films: part 1. The influence of fabrication governed surface conditions, *J. Mech. Phys. Solids*, 51, 2003, pp. 1533–1550.

[21]. Sharpe W. N., Brown J. S., Johnson G. C., Knauss W. G., Round-robin tests of modulus and strength of polysilicon, *Materials Research Society Proceedings*, San Francisco, CA, Vol. 518, 1998, pp. 57–65.